

FIN AND REAR STINGS SUPPORT EFFECTS ON THE FLOW AROUND THE AIRCRAFT MODEL

S.A. Glazkov, A.R. Gorbushin, I.A. Kursakov
TsAGI, Russia

Keywords: *sting interference, fin and rear stings, dummy fin and rear stings*

Abstract

The paper is devoted to solving one of the most important problems of testing aircraft models in wind tunnels – to influence of supporting devices upon flow around models.

The current paper presents the results of numerical and experimental investigations of rear and fin sting influence on aerodynamic characteristics of aircraft model in wind tunnel T-128 (TsAGI).

1 Introduction

During the tests in wind tunnels, aircraft models are mounted on different types of supporting devices. Therefore, the conditions of experiment differ from real free flight condition. Supporting devices produce flow perturbations in zones around model and, hence, distort aerodynamic characteristics of tested models. Besides, the model geometry changes according to the type of supporting device. It has to be taken into account too. Experimenters have two main problems concerning the influence of supporting devices:

- to design a supporting device that produces minimal influence on aerodynamic characteristics of model;
- to determine interference of support system and to correct experimental results.

Influence of supporting device is under investigation in many research centers. Thus, in the paper [1], investigation results of influence of rear and Z-shape stings are presented for ONERA.

Influence of supporting device can be determined both in experiment [2] and using fast-developing numerical methods [3].

For numerical estimations of supporting device influence, two methods are used at TsAGI:

- panel method;
- numerical solutions of Reynolds-averaged Navier-Stokes equations with the use of EWT software package [3].

The calculations have been performed for the same configurations of model as have been used in tests. At that, integral parameters of support interference, such as correction to Mach number of free stream flow and correction to angle of attack, have been used. Corrections to coefficients of aerodynamic forces and moments have been calculated.

Obtained corrections are presented as functional dependence on main flow parameters.

A method of experimental data correction is described. Proposed procedures are demonstrated with the used of data obtained in numerical experiment (EWT calculations).

2 Experimental investigations

2.1 T-128 wind tunnel

Wind tunnel T-128 is a closed circuit continuously running facility with variable density of air [2]. Test section, where model and mixing chamber (reentry zone) are placed, is a single structural component. It is usually named as interchangeable test section. Length of test section is 12 m. Size of cross-section at the entrance is 2.75 m × 2.75 m, Size of cross-section at the exit is 2.75 m × 3.5 m.

Wind tunnel T-128 is equipped by four interchangeable test sections. Test section №1 is

intended for investigation of full aircraft models mounted at rear and fin stings. Model incidence and slip angles can be changed, Mach number is in the range from $M_\infty=0.15$ to $M_\infty=1.7$. Rear sting is fixed in crescent -shaped rigid support that is mounted, in turn, to mechanism for its shifting. Range of mechanism pitching angle is $\alpha = \pm 30^\circ$, yaw angle is $\beta = \pm 15^\circ$.

Test section №1 has adjustable perforated panels; perforation coefficient can be changed separately for each panel. It is in the range from 0% to 18%.

2.2 Fin and rear stings and their dummy stings

Influence of two main types of supporting devices (fin and rear stings) was investigated by method of their doubling. During the investigation of rear sting, model tests have been performed on the fin sting with dummy of rear sting (Fig. 1) and without it.



Fig.1. Fuselage + Wing mounted on fin sting with dummy of rear sting

To investigate fin sting interference, model tests have been performed on rear sting with dummy of fin sting (Fig. 2) and without it.



Fig.2. Fuselage+Wing +Horizontal Tail at rear sting with dummy of fin sting

Configuration of new optimal fin (NOF) sting for testing the model RRJ-95 was presented in paper [3]. Form of fin sting has been designed so as geometry of model vertical tail is reproduced as exact as possible (in terms of leading edge sweep and root profile).

Tests in T-128 wind tunnel have been performed for the following configurations of model: isolated fuselage (F); F+wing (W); F+W+horizontal tail (HT); F+W+HT+vertical tail (for rear sting only).

Model tests have been performed for Mach numbers $M_\infty=0.7$, 0.8 and 0.88 with fixed laminar-turbulent transition of boundary layer. Transition has been fixed using the strip of disks with height 0.1 mm installed at $x_{II}=3\%$ on the fuselage and at $x_{II}=10\%$ on wing, horizontal and vertical tails. Forward position of transition was chosen because turbulent boundary layer was used in calculations.

3 Numerical investigations

3.1 Panel method

In framework of linear potential theory, many results are obtained either in explicit form (in quadratures) or in fast-realized numerical solutions. It permits fast estimation of phenomena.

Flow around aircraft or its elements (separately) is assumed to be ideal compressible inviscid gas (compressibility is taken into account according to Prandtl-Glauert rule). It is the problem formulation, which quite corresponds to aims of far field investigation in the case of flow around sting. Figure 3 presents surface discretization for the calculation of flow around isolated fuselage and fuselage with fin sting using panel method. Grids for isolated fuselage and for fuselage with sting were the same.

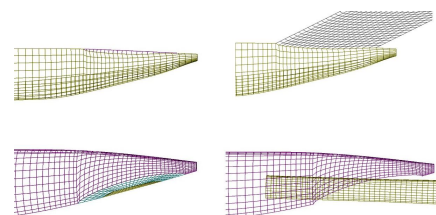


Fig.3. Surface discretization of fuselage rear part with fin and rear stings

In calculation of flow around the isolated fuselage, flow parameters at the regions of the virtual wing and horizontal tail were computed. Figure 4 (variant with fin sting) demonstrates them by the green and blue colors correspondingly. Flow parameters in these regions are compared for the cases with and without sting; it permits to estimate flowfield distortion produced by supporting device.

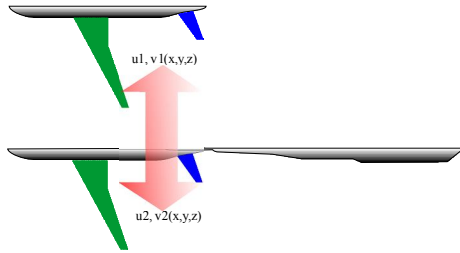


Fig.4. Virtual surfaces of wing and horizontal tail, where flow parameters are compared

3.2 Software package EWT TsAGI

The calculations have been performed with use of software package EWT-TsAGI [4]. The main characteristics of this package are following:

- structured calculation grid;
- explicit and implicit TsAIG's scheme based on Godunov-Kolgan-Rodionov scheme (GKR);
- Euler, Navier-Stokes and Reynolds equation systems;
- TsAGI's turbulence models based on q- ω , SST, SA models;
- method of large eddy simulation (LES);
- stationary and non-stationary solvers;
- fractional time step;
- code for calculation of engine jet acoustics;
- MPI, multithreading.

The current paper uses implicit GKR scheme [5] to solve Reynolds equation system (solver COMGLEI). For closure this equation system, SST turbulence model is used. The mathematical model for the task considered was developed with a necessity to vary the supporting devices taken into account. As a result, a special toolset has been designed to permit adjustment of geometrical parameters and grids.

The procedure of preparing the calculation grid has been divided into some stages:

- Dividing the total computational domain into subregions with independent topologies;
- Creation of grid topology for each subregion;
- Combination of subregions and generation of whole space calculation grid.

Figure 5 presents the calculation grid structure for model configuration of fuselage + wing + horizontal tail at rear sting with dummy of fin sting. Flow calculations have been performed for all configurations.

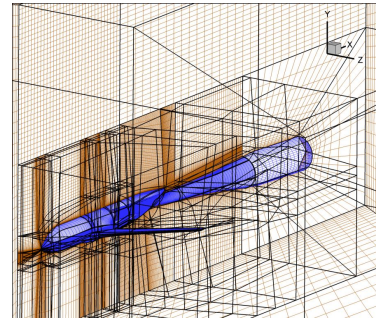


Fig.5. Block structure of grid for configurations of fuselage + wing models with rear sting

4 Calculation or corrections for influence of supporting devices

Different elements of aircraft model are subjected by the influence of supporting devices to a variable extent. For example, aerodynamic force coefficients (ADF) of the passenger aircraft wing (or horizontal tail) are very sensitive to changes of incidence angle and free stream flow velocity (Mach numbers), while, in the case of fuselage, aerodynamic coefficients are more conservative:

$$\frac{\partial CL_{fus}}{\partial \alpha} \ll \frac{\partial CL_{wing}}{\partial \alpha} \quad \frac{\partial CD_{fus}}{\partial \alpha} \ll \frac{\partial CD_{wing}}{\partial \alpha}$$

$$\frac{\partial CL_{fus}}{\partial M} \ll \frac{\partial CL_{HT}}{\partial M} \quad \frac{\partial CD_{fus}}{\partial M} \ll \frac{\partial CD_{HT}}{\partial M}$$

Because of fuselage length, longitudinal gradients of velocity caused by supporting devices have dominant influence on fuselage characteristics. These circumstances are to be taken into account while choosing methods of determining corrections the influence of supporting devices.

4.1 Corrections for main flow parameters

Several methods were used to solve fin sting interference problem:

- 1) In the frames of linear aerodynamics, using calculations of far field around isolated fin sting to determine mean parameters of disturbed flow velocity ΔM_{wing} , and upwash $\Delta\alpha_{wing}$ for the wing and for the horizontal tail ΔM_{HT} , $\Delta\alpha_{HT}$. Corrections to the forces acting on the fuselage (ΔCD_{fus} , ΔCL_{fus} , ΔCpm_{fus}) are calculated by integrating pressure induced by sting over fuselage surface.
- 2) On basis of calculations (panel method or EWT) of flow around two configurations (fuselage and fuselage + fin sting), flow distortion induced by supporting device near virtual surfaces (wing, horizontal tail) is determined and averaged parameters ΔM_{wing} , $\Delta\alpha_{wing}$, ΔM_{HT} , $\Delta\alpha_{HT}$ are calculated. Comparing aerodynamic coefficients of two configurations, one may determine corrections: ΔCD_{fus} , ΔCL_{fus} , ΔCpm_{fus} .

General scheme of corrections determination is presented in Fig. 6.

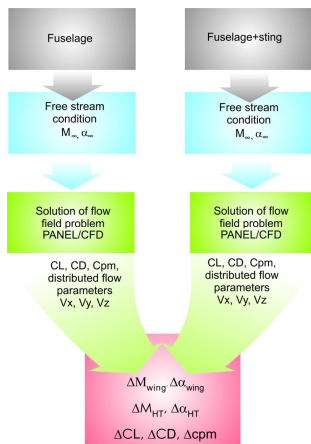


Fig. 6. General scheme for calculation of sting interference parameters and for correction of aerodynamic coefficients

Integral corrections for Mach number (ΔM) of free flow and for incidence angle ($\Delta\alpha$) within investigated velocity range, in the case of fin sting, have been calculated as follows:

1. Blockage $\Delta M_{1/4} = \frac{1}{S} \int \Delta M_{1/4}(z)b(z)dz$ and

$$\Delta M = \frac{1}{S} \iint_S \Delta M(x, y, z)ds, \text{ where } \Delta M_{1/4}(z) \text{ is}$$

local perturbation of Mach number produced by sting along the line at $1/4$ wing chord $b(z)$.

2. Upwash is averaged similarly to blockage:

$$\Delta\alpha_{3/4} = \frac{1}{S} \int \Delta\alpha_{3/4}(z)b(z)dz \text{ and}$$

$\Delta\alpha = \frac{1}{S} \iint_S \Delta\alpha(x, y, z)ds$, where $\Delta\alpha_{3/4}$ is a local upwash produced by the sting along the line of $3/4$ wing chord.

These are, correspondingly, two methods of averaging the non-uniform perturbation - averaging along the line of $1/4$ chord for ΔM ($3/4$ chord for $\Delta\alpha$) and averaging over the surface. Figure 7 presents the distribution of upwash (in degrees) and blockage (in terms of Mach number), caused by fin sting, near wing for regime $M_\infty=0.8$ and $\alpha=2.5^\circ$. Presented distributions show rather weak gradients of perturbations. For example, in the case of upwash, deviations from averaged value don't exceed the value $\sim 0.006^\circ$ and, in the case of blockage, $\delta(\Delta M) \sim 0.0005$.

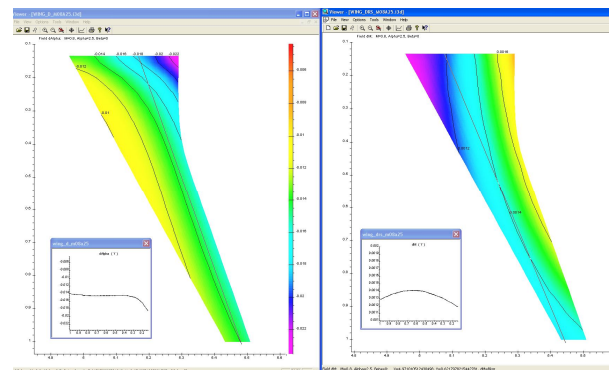


Fig. 7. Distributions of upwash and blockage near wing because of fin sting effect

Following results have been obtained:

- I. Integral corrections of free flow parameters due to sting influence obtained by two numerical methods (PANEL/EWT) differ slightly: $\delta[\Delta\alpha] < 0.003^\circ$; it diminishes noticeably with growth of free flow Mach number; $\delta[\Delta M] < 0.0005$; it diminishes with decrease of free flow Mach number;
- II. Vertical tail doesn't influence on integral correction over the wing.
- III. Estimation of integral corrections using far field calculations (panel method), in the case of flow around isolated fin and rear sting, has not great error: $\delta[\Delta\alpha] < 0.005^\circ$ – essentially dimin-

ishes with growth of free flow Mach number; $\delta[\Delta M] < 0.0004$ – doesn't depend on free flow Mach number;

IV. The difference between two methods of averaging perturbed parameters of flow is small and not more than: $\delta[\Delta \alpha] < 0.003^\circ$; $\delta[\Delta M] < 0.0003$.

There is no essential difference between two averaging methods because there are no essential gradients in upwash and longitudinal velocity component caused by stings.

4.2 Corrections to aerodynamic coefficients

Within the range of investigated regimes $0.7 \leq M_\infty \leq 0.88$ and $-1.25^\circ \leq \alpha \leq 2.5^\circ$, linear and quadratic functional dependencies on free flow parameters M_∞ и α_∞ have been obtained for corrections using performed calculations (EWT-TsAGI) for fin and rear sting configurations.

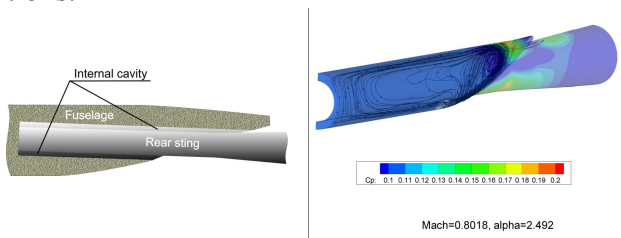


Fig. 8. Scheme of coaxial cavity near model-sting connection zone and flow structure in it (fuselage + rear sting configuration, $M_\infty=0.80$, $\alpha=2.492^\circ$)

In the case of fin sting, there is no cross-flow in the zone of model-sting connection (it takes place "by definition" in calculations and it is due to the sealing in the experiment). In the case of rear sting, the flow has a complicated structure in the coaxial cavity near model-sting connection zone (see Fig. 8). In the face of cavity, gas has practically zero velocity and there are intense vortices above the sting at tail part of fuselage.

Pressure distribution at the section $x=2.13$ m is presented in Fig. 9 for two configurations: fuselage + rear sting and F+W+rear sting. In the case of negative incidence angle $\alpha=-1.254^\circ$, the difference is small and, in the case of $\alpha=2.492^\circ$, there is growth of stagnation zone size at windward side of rear sting and diminishing the acceleration zone at lateral side of

rear sting. As a result, pressure changes in the cavity.

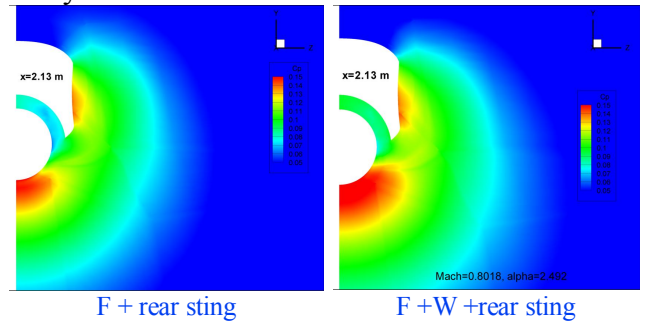


Fig. 9. Comparison of pressure distribution at the section $x=2.13$ m for configurations of fuselage + rear sting and fuselage + wing + rear sting, $M_\infty=0.8018$, $\alpha=2.492^\circ$

Total representation about distribution of forces acting on the cavity surface can be obtained from the results presented in Fig. 10 for fuselage + rear sting configuration at different incidence angles $\alpha=-1.25^\circ$ and 2.5° and free flow Mach number $M_\infty=0.80$. It should be noted an important circumstance – quick stabilization of pressure inside the cavity. There are strong pressure gradients near overhang of convergent tail of fuselage above the sting (it is shown in Figure 10 by the red color). The arrow shows the place of application of total force that acts on the cavity.

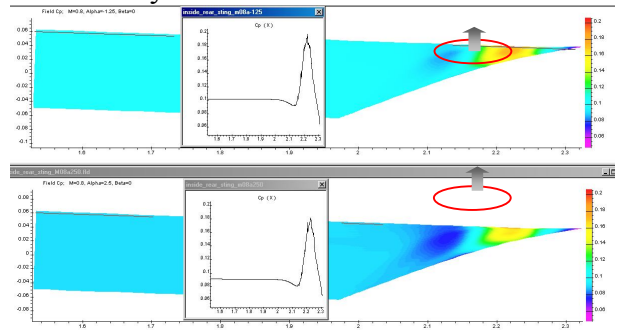


Fig. 10. Distribution of C_p over coaxial cavity near model-sting connection zone of fuselage at $M_\infty=0.8$ and incidence angles $\alpha=-1.25^\circ$, 2.5°

The balance measures a total load $\vec{F}_{balance} = \vec{F}_{AF}^S + \vec{F}_{CAV}^S + \vec{F}_F^S$:

- force F_{AF}^S acting on the outer surface of model frame (sum of pressure and friction forces) – it is aerodynamic force under investigation without taking into account the sting cutout surface;
- pressure force F_{CAV}^S acting on the face of inner coaxial cavity (friction forces are

absent), - it is base drag;

- pressure force F_F^S acting on the cylindrical surface of coaxial cavity (friction forces are negligible).

The result obtained in the experiment with rear sting, according to traditional methodology, is following: $\vec{F}_{WT} = \vec{F}_{balance} - \vec{F}_{CAV} = \vec{F}_{AF}^S + \vec{F}_F^S$. It is obvious that the present approach in balance experiment doesn't take into account loads over internal model cavity (in our case, it is a cylindrical surface of cavity).

So, to obtain real model load \vec{F}_{REAL} , in the case of free flow without supporting devices, it is necessary:

1. to estimate the force \vec{F}_F^S ;
2. to correct the force \vec{F}_{AF}^S taking into account the influence of supporting devices $\vec{F}_{AF}^S \longrightarrow \vec{F}_{AFCOR}^S$.

Then, using the experimental results \vec{F}_{WT} and taking into account the foresaid, one can obtain $\vec{F}_{REAL} = (\vec{F}_{WT} - \vec{F}_F^S)_{COR} = \vec{F}_{AFCOR}^S$.

Using the results of performed calculations, functional dependencies of additional corrections to aerodynamic force coefficients (for experiments with rear sting) were obtained: $\Delta CL_{fus}^{CAV} = 0.0055M_\infty - 0.0002\alpha + 0.0047$;

$$\Delta CD_{fus}^{CAV} = \Delta CL_{fus}^{CAV} \sin(\alpha); \quad \Delta Cpm_{fus}^{CAV} = -4.78\Delta CL_{fus}^{CAV}.$$

5 Correction of experimental results

The procedure of experimental data correction for influence of supporting devices depends on investigated model configuration, in accordance with considerations from the previous Section. The presented materials have been obtained during the numerical simulation (see Section 3.2).

5.1 Isolated fuselage

Free flow parameters for tests of isolated fuselage and fin sting correspond to the values required in test program. Corrections obtained from comparison of two configurations (fuselage and fuselage + fin sting) are added to the coefficients of aerodynamic forces obtained in the experiment:

$$C^{COR}(M, \alpha) = C^{STING}(M, \alpha) + \Delta C_{fus}(M, \alpha); \quad \text{where} \\ C = CL; CD; Cpm.$$

If rear sting is used, then:

$$C^{COR}(M, \alpha) = C^{STING}(M, \alpha) + \Delta C_{fus}(M, \alpha) + \Delta C_{fus}^{CAV}(M, \alpha).$$

5.2 Model configuration – F+W

Free flow parameters for test of fuselage + wing on fin sting configuration:

M_∞^S is free flow Mach number; α_∞^S is free flow incidence angle. They are determined as follows: $M_\infty^S = M_\infty - \Delta M_W$, where M_∞ is free flow Mach number that corresponds to flow without supporting devices, ΔM_W is the value that characterizes flow deceleration near wing produced by supporting devices; $\alpha_\infty^S = \alpha_\infty + \Delta\alpha_W$, where α_∞ is free flow incidence angle that corresponds to flow without supporting devices, $\Delta\alpha_W$ is the value that characterizes flow deflection near wing produced by supporting devices. In the experiment with a given Mach number M_∞^S , flow over the wing has velocity, which practically corresponds to Mach number M_∞ , and, correspondingly, dynamic pressure $Q^C = Q^{exp} \left(1 + \frac{\Delta Q}{Q}\right)$, where

$$\frac{\Delta Q}{Q} = \frac{\Delta M_W}{M_\infty^S} \frac{(2 - M_\infty^{S^2})}{(1 + 0.2M_\infty^{S^2})}. \quad \text{Correspondingly, corrected pressure coefficient over the model surface is following:}$$

is following:

$$c_p^C(x) = c_p^{exp}(x) - c_p^{exp}(x) \frac{\Delta Q}{Q} + \frac{2\Delta M_W}{M_\infty(1 + 0.2M_\infty^2)}.$$

With taking into account the modified dynamic pressure and corrections for aerodynamic force coefficients, corrected data have following form:

$$CD^C(M_\infty, \alpha_\infty) = CD^S(M_\infty^S, \alpha_\infty^S) \left(1 - \frac{\Delta Q}{Q}\right) + CL^S(M_\infty^S, \alpha_\infty^S) \sin(\Delta\alpha_W) + \Delta CD_F(M_\infty^S, \alpha_\infty^S); \\ CL^C(M_\infty, \alpha_\infty) = CL^S(M_\infty^S, \alpha_\infty^S) \left(1 - \frac{\Delta Q}{Q}\right) + \Delta CL_F(M_\infty^S, \alpha_\infty^S); \\ Cpm(M_\infty, \alpha_\infty) = Cpm^S(M_\infty^S, \alpha_\infty^S) \left(1 - \frac{\Delta Q}{Q}\right) + \Delta Cpm_F(M_\infty^S, \alpha_\infty^S).$$

When the rear sting is used, then, as in the case of isolated fuselage, additional forces acting on

the cavity in the fuselage are taken into account.

Figure 11 presents fragments of pressure distribution at some sections ($z=0.4, 0.6, 0.8$ m) over the wing of investigated model.

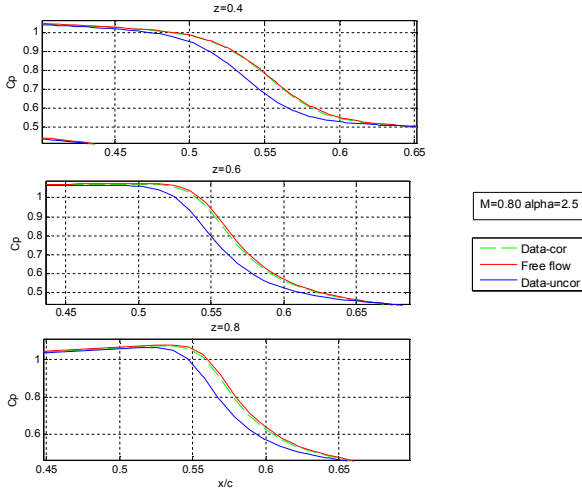


Fig. 11. Comparison of pressure distributions over the model wing (near the shock wave) at some sections with and without fin sting; corrected data for the model at fin sting

Three variants of flow at regime that is close to cruising one (EWT calculations) are compared: 1) flow around fuselage + wing + fin sting configuration at $M_{cor\infty}=0.8014$ and $\alpha_{cor\infty}=2.518^\circ$, pressure coefficient c_p has also been corrected (the green line in plot); 2) flow around fuselage + wing configuration at $M_\infty=0.8$ and $\alpha_\infty=2.5^\circ$ - without sting (the red line in plot); 3) flow around fuselage + wing + fin sting configuration at $M_\infty=0.8$ and $\alpha_\infty=2.5^\circ$ (the blue line in plot).

Sting influence is the most obvious as the effect of flow deceleration near the wing. As a result, the shock shifts upstream (blue curve as compared to red curve in plots - Fig. 11). This displacement is $\sim 2\%$ of chord. After correction of flow parameters and pressure coefficients (taking into account the dynamic pressure), flow around the wing with the sting becomes practically the same as without supporting device. The difference of pressure coefficient doesn't exceed $\Delta c_p \leq 0.003$.

The results of pressure distribution correction over the wing, in the case of model at rear sting, also remove the interference.

The introduced correction of free flow pa-

rameters permits to remove practically sting influence on flow around the wing.

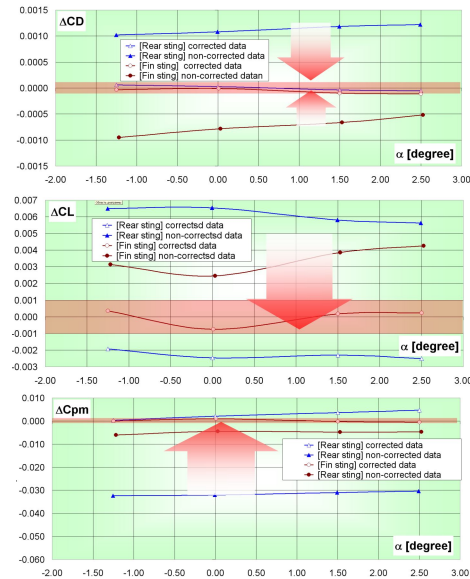


Fig. 12. Comparison of differences of non-corrected and corrected data with free flow (without supporting devices), $M_\infty=0.8$

Figure 12 presents calculated differences of aerodynamic force coefficients over the model with stings (with taking into account the corrections for influence of fin and rear stings and without these corrections) at $M_\infty=0.8$. The corrections of total loads over the model have permitted to diminish the difference between corrected data and the results of free flow without a sting:

for fin sting: drag - to $|\Delta CD| \leq 0.0001$; lift - to $|\Delta CL| \leq 0.001$; pitching moment - to $|\Delta Cpm| \leq 0.0015$;
for rear sting: drag - to $|\Delta CD| \leq 0.0002$; lift - to $|\Delta CL| \leq 0.003$; pitching moment - to $|\Delta Cpm| \leq 0.004$.

5.3 Model configuration – F+W+HT

Similarly to F+W configuration, corrections to free flow parameters were defined taking into account the distortion of flowfield near HT: $\Delta^c M_{HT} = \Delta M_{HT} - \Delta M_W$;

$$\Delta^c \alpha_{HT} = \Delta \alpha_{HT} - \Delta \alpha_W.$$

The difference between corrected data and results of free flow without sting is essentially greater than for F+W configuration, especially for rear sting. It is, most likely, due to interference of horizontal tail and the sting. In the case

of rear sting, this effect is stronger, because the cutout at tail part of the fuselage is near HT.

In terms of total model loads, the corrections have permitted to diminish the difference between corrected data and results of free flow without sting:

for fin sting: drag - to $|\Delta CD| \leq 0.0004$; lift - to $|\Delta CL| \leq 0.0035$; pitching moment - to $|\Delta Cpm| \leq 0.01$;

for rear sting: drag - to $|\Delta CD| \leq 0.0002$; lift - to $|\Delta CL| \leq 0.01$; pitching moment - to $|\Delta Cpm| \leq 0.01$.

6 Determination of fin and rear sting influence using the experimental investigation results by doubling method

Experimental corrections are determined by comparing the aerodynamic coefficients (lift, drag and pitching moment) with and without dummy. For example, using the results of two types of experiment [2]:

- 1 fuselage on the rear (fin) sting with dummy of fin (rear) sting;
- 2 fuselage on rear (fin) sting.

Similarly, for all investigated configurations, we have $\Delta C(\alpha_\infty, M_\infty) = C^{dummy-} - C^{dummy+}$.

And, correspondingly, we can obtain corrected data from correction determination: $C^C(\alpha_\infty, M_\infty) = C^{S+}(\alpha_\infty, M_\infty) + \Delta C(\alpha_\infty, M_\infty)$

Analogue of these corrections (for isolated fuselage) has been obtained using numerical simulation of investigated model in Section 4.

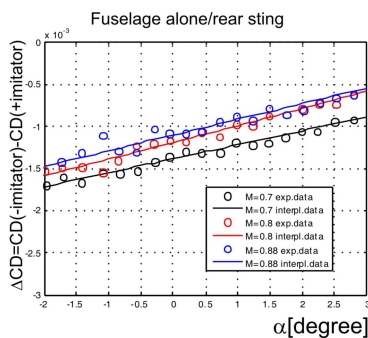


Fig.13. Influence of fin sting dummy on fuselage drag

For example, Figure 13 shows the plots of fin sting dummy influence on drag coefficient ΔCD versus incidence angle α . Influence functions that have been obtained as a result of linear interpolating the experimental

data by the least-squares method are presented in analytical form: $\Delta CD = a_1\alpha + a_0$; $\Delta CL = b_1\alpha + b_0$; $\Delta Cpm = c_1\alpha + c_0$. They have been used for correction of experimental data.

7 Comparison of numerical simulation and experimental investigation results

Performed comparisons of steady pressure values in the cavity of the model mounted on the rear sting have shown that calculated data are in qualitative correspondence with the experiment. The difference isn't more than ~12%, it corresponds to the difference of base drag ≤ 0.0002 .

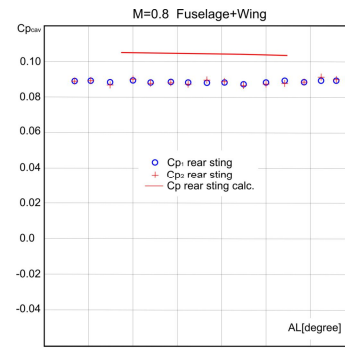


Fig.14. Base pressure for fuselage +wing configuration, $M_\infty=0.8$

For example, Figure 14 presents data for fuselage +wing configuration at $M=0.8$. Probably, to improve the coincidence of numerical and experimental data, it is necessary to simulate the shape of cavity in the model in more detail.

In correspondence with recommendations of Sections 3-5, corrections for influence of supporting devices have been introduced into the experimental results of the model at fin and rear stings. They are two types of corrections:

- "numerical", obtained from the numerical simulation results;
- "experimental" - on basis of experimental data (doubling method described in Section 6).

Comparison of corrections of aerodynamic force and moment coefficients for isolated fuselage is presented in Fig. 15.

In order to increase the scale of the plots linear functions were subtracted from lift and pitching moment coefficients $CL^* = CL - (b_0 + b_1 AL)$ $Cpm^* = Cpm - (c_0 + c_1 AL)$ and squared relationship was subtracted from drag coefficient $CD^* = CD - (a_0 + a_1 AL + a_2 AL^2)$.

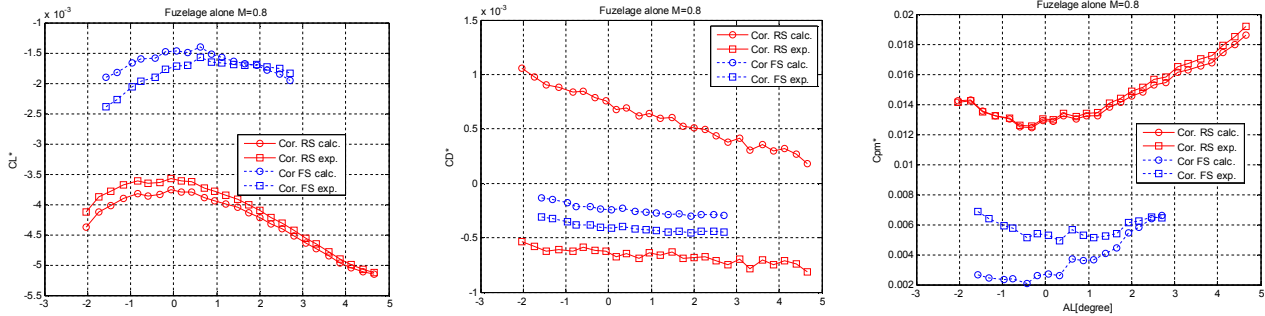


Fig. 15. Corrected aerodynamic coefficients for fuselage configuration, $M_\infty=0.8$

Corrections to the lift coefficient ΔCL for fin and rear stings have different signs. It is due to positions of supporting devices with respect to fuselage axis. The rear sting is under the fuselage axis and inclined at the angle of 2° . Fin sting is above the fuselage. Within the whole investigated range of incidence angles and velocities, difference between numerical and experimental corrections doesn't exceed 0.0005 for both stings (in Figures, fin sting is denoted by symbols - FS, and the rear sting - RS). Corrected data for both stings differ not more than 0.0025. Corrections to pitching moment ΔCpm correspond to lift corrections. As for rear sting, difference between numerical and experimental corrections doesn't exceed ~ 0.001 . Their value is visibly higher than corrections obtained for fin sting. Difference between numerical and experimental corrections, in the case of fin sting, at incidence angle $\alpha = -1.5^\circ$ is about ~ 0.004 and diminishes to almost zero at $\alpha = 3^\circ$ with growth of incidence angle. Corrected data for both stings differ not more than 0.012. Corrections to lift and pitching moment slightly depend on free flow velocity within investigated range. Absolute values of numerical corrections of fuselage drag coefficient for fin sting case is rather less than experimental ones. The difference at $M=0.8$ doesn't exceed ~ 0.00015 . Numerical and experimental corrections, in the case of rear sting, have different signs. This difference is quite noticeable: from ~ 0.0007 to ~ 0.0015 . It diminishes with growth of

incidence angle. It can be caused by insufficient accuracy of simulating of the form of cavity at the fuselage tail part where the sting is inserted.

It is interesting to compare the corrected data for different stings. For example, maximal difference of corrected lift coefficients is about ~ 0.002 for $M_\infty=0.7, 0.8$ and slightly higher at $M_\infty=0.88$ - ~ 0.003 . Difference of pitching moments is essential (~ 0.01). It is explained by large arm of even inessential lift force.

Comparison of data with and without corrections for F+W configuration is presented in Fig. 16. In order to increase the scale of the plot linear function was subtracted from angle of attack $ALT = \alpha - kCL$. Maximal difference between corrected lift coefficient $CL(ALT)$ for two sting configurations, in terms of incidence angle, is about $\sim 0.05^\circ$ at $CL=0.5$ and is even less ($\sim 0.03^\circ$) if only numerical corrections are considered.

The best coincidence of numerical and experimental corrections have been obtained for pitching moment coefficient for both stings. In the case of rear sting, corrected pitching moment coefficients are higher by 0.015 by average. At that, they are practically parallel unlike non-corrected data. As a whole, model drag after applying the corrections for influence of supporting devices diminishes, but corrected drag values obtained for different types of sting don't coincide. The difference between experimental data with experimental corrections for different type of sting is

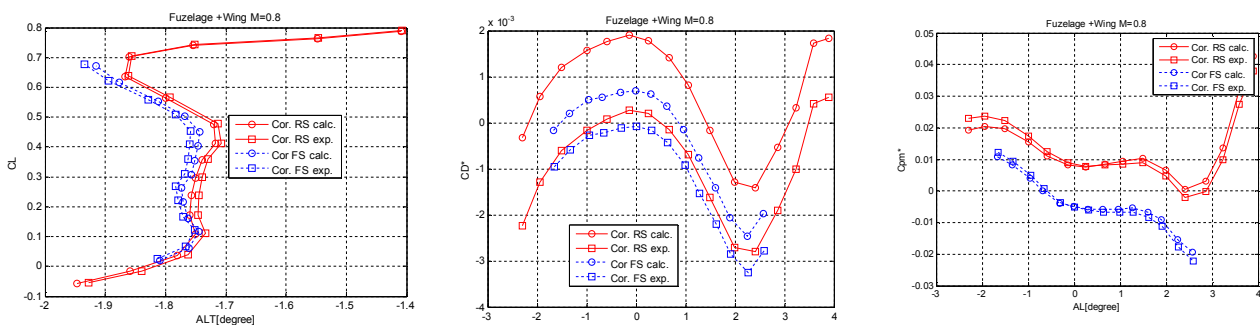


Fig. 16. Corrected aerodynamic coefficients for fuselage+wing configuration, $M_\infty=0.8$

about $\sim 0.0002 \div 0.0003$ at $M_\infty = 0.8$. Difference between two correction methods for fin sting is about ~ 0.0008 .

Comparison for F+W+HT configuration is presented in Fig. 17. As a whole, all tendencies remain as for fuselage + wing configuration. The difference between experimental data with experimental corrections for different type of stings for CL(AL) at CL=0.5 is about $\sim 0.03^\circ$. Data corrected using numerical method for fin sting are essentially underestimated. Similar situation is for pitching moment coefficient. Data for rear sting that have been corrected using two methods well correlate between each other – the difference doesn't exceed ~ 0.008 . Data for the fin sting that have been corrected using experimental method are rather higher (by $+0.005$), and data for the fin sting that have been corrected using numerical method are essentially higher. After introducing corrections for influence of supporting devices, the model drag diminishes. The difference between data with experimental corrections for two stings is about ~ 0.0004 . The difference of two correction methods for fin sting doesn't exceed 0.001.

In conclusion, it should be noticed that, for providing the possibility of the model mounting on the stings of different types, there were some variants of model stern. In additions, some defects of model manufacturing are possible. All these phenomena can be a reason of difference between corrected loads, because, in fact, the model stern form could be varied from one sting to another.

It should be mentioned that there is interference between the sting and dummy and, generally speaking, the results of numerical and experimental corrections haven't to coincide absolutely.

References

- [1] Aurelia Cartieri, S. Mouton, G. Boyet Study of support interference effects at S1MA wind tunnel within the "SAO" project, *ICAS 2010*, Brisbane, Australia.
- [2] S.A. Glazkov, A.R. Gorbushin, N.N. Khoziaenko, T.V. Konotop, V.A. Terekhin Investigation of the rear support interference on the aerodynamic characteristics of the RRJ-95 model in the T-128 transonic wind tunnel, *21st International Congress On Instrumentation in Aerospace Simulation Facilities*, August 29th –September 1st, 2005, Sendai International Center Sendai, Japan.
- [3] S.L. Chernyshev, V.Ya. Neyland, S.M. Bosnyakov, A.R. Gorbushin, S.A. Glazkov, I.A. Kursakov, V.V. Vlasenko Experience in the application of numerical methods to TsAGI's wind-tunnel testing techniques, *5th Symposium on Integrating CFD and Experiments in Aerodynamics* (Integration 2012) 3-5 October 2012 JAXA Chofu Aerospace Center, Tokyo, Japan.
- [4] S. Bosnyakov, V.Neyland, I. Kursakov, V. Vlasenko, S. Matyash, S. Mikhayalov, J. Quist Experience of CFD data implementation for preparation and performing wind tunnel test, *Mathematical modeling*, v. 25, №9, 2013.
- [5] Coakley T., Hsieh T. Comparison between implicit and hybrid methods for the calculation of steady and unsteady inlet flows, *AIAA-85-1125*, 1985.

8 Contact Author Email Address

A.R. Gorbushin: gorbushin@tsagi.ru

Copyright Statement

The authors confirm that they, and/or their company or organization, hold copyright on all of the original material included in this paper. The authors also confirm that they have obtained permission, from the copyright holder of any third party material included in this paper, to publish it as part of their paper. The authors confirm that they give permission, or have obtained permission from the copyright holder of this paper, for the publication and distribution of this paper as part of the ICAS 2014 proceedings or as individual off-prints from the proceedings.